Aura Microwave Limb Sounder observations of the Northern Annular Mode: From the mesosphere to the upper troposphere

Jae N. Lee,[1] Dong L. Wu,[1] Gloria L. Manney,[1,2] and Michael J. Schwartz[1]

Received 29 August 2009; revised 22 September 2009; accepted 24 September 2009; published 30 October 2009.

[1] Vertical structure and evolution of the wintertime Northern Hemisphere Annular Mode (NAM), the first Empirical Orthogonal Function (EOF) of geopotential height anomalies, are constructed from the 2005–2009 Aura Microwave Limb Sounder (MLS) measurements in the entire middle atmosphere between 316 hPa (∼9 km) and 0.001 hPa (∼90 km). This is the first report of NAM structure extending into the mesosphere. The mode appears to be robust and it accounts for up to 70% of middle-atmospheric variance before decreasing in the upper mesosphere. The vertical connection of the NAM modes suggests strong dynamic coupling between the mesosphere and stratosphere. Time evolution of the NAM suggests that the significant NAM anomalies typically appear first in the mesosphere and progress downward. NAM patterns derived from MLS observations are consistent with those derived from long-term reanalysis below the middle stratosphere. The NAM indexes show the mesospheric cooling signals during the major stratospheric sudden warmings (SSWs) in 2006 and 2009. **Citation:** Lee, J. N., D. L. Wu, G. L. Manney, and M. J. Schwartz (2009), Aura Microwave Limb Sounder observations of the Northern Annular Mode: From the mesosphere to the upper troposphere, *Geophys. Res. Lett.*, *36*, L20807, doi:10.1029/2009GL040678.

1. Introduction

[2] The Northern annular mode (NAM), an approximately axially symmetric perturbation of hemispheric geopotential height (GPH) relative to that of mid-latitudes, is an important tool for diagnosing variability of the winter polar atmosphere [*Thompson and Wallace*, 1998, 2000]. The vertical coherence of the winter NAM pattern plays a fundamental role in the stratosphere-troposphere coupling, both in observations [e.g., *Baldwin and Dunkerton*, 1999, 2001; *Black*, 2002] and in model simulations [e.g., *Limpasuvan and Hartmann*, 2000; *Plumb and Semeniuk*, 2003; *Kushner and Polvani*, 2004; *Hardiman and Haynes*, 2008].

[3] Polar stratosphere-to-troposphere coupling events are often preceded by a disturbance in the upper atmosphere [*Baldwin and Dunkerton*, 1999]. *Sherhag et al.* [1970] show that the signs of SSWs begin as high as 60 km and progressed downward. Recent observations show that mesospheric cooling and MLT (mesosphere and lower thermosphere) zonal wind reversals occur prior to the SSWs [e.g., *Hoffmann et al.*, 2002; 2007; *Manney et al.*, 2008, 2009a]. Interactions between the upper and middle atmospheres are complex and multifold. For example, transport of *NO* and NO_2 from the mesosphere is the major driver for catalytic ozone loss in the mid stratosphere [*Brasseur and Solomon*, 2005]. *Lahoz et al.* [2009] show that the large-scale features in potential vorticity (PV) in the upper stratosphere/lower mesosphere are correlated with methane cross-sections, suggesting that large scale dynamics plays an important role in transport of tracers.

[4] Historically, observations have been limited to the altitudes below the stratopause (most below the middle stratosphere) because high-altitude data have not been available, and meteorological analyses become progressively more unreliable above the middle stratosphere [e.g., *Manney et al.*, 2008]. Satellite instruments like Aura MLS can help fill in this gap in the observational record, and in meteorological analyses. Here, we use Aura Microwave Limb Sounder (MLS) GPH data to derive the structure of the winter NAM and other leading EOF modes from the upper troposphere through the mesopause. These results are also used to study the mesosphere (up to 0.001 hPa)-stratosphere (10–0.046 hPa) coupling during the major SSWs in 2006 and 2009 [e.g., *Manney et al.*, 2008, 2009a, 2009b] by focusing on the new results above the stratosphere.

2. Data and Methods

[5] The data used in this study are the version 2.2 (v2.2) daily GPH from Aura MLS, launched in July 2004, which provides a GPH retrieval on 35 pressure levels from the upper troposphere (316 hPa) through the mesopause (∼0.001 hPa). The MLS GPH measurement error generally increases with height during the boreal winter, estimated to be 100 m or less for 10 hPa to 0.046 hPa, and 500–750 m at 0.001 hPa. Details on validation of the MLS geopotential height field are discussed by *Schwartz et al.* [2008].

[6] We adopt *Baldwin and Dunkerton*'s [1999, 2001] method to calculate the NAM indexes. The MLS GPH field is mapped into 4 (latitude) × 8 (longitude) grid cells from the average of daily ascending and descending orbits. A winter time (DJF) mean over the five years of MLS GPH observation has been removed at each grid cell at a given altitude to calculate the daily GPH anomalies at each MLS retrieval level. GPH anomalies are multiplied by the square root of cosine of latitude from 20N to 84N to yield area-weighted variances in each grid cell. The NAM is defined as the first EOF of the temporal covariance matrix

[1]Jet Propulsion Laboratory, California Institute of Technology, Pasadena, California, USA.
[2]New Mexico Institute of Mining and Technology, Socorro, New Mexico, USA.

0094-8276/09/2009GL040678$05.00

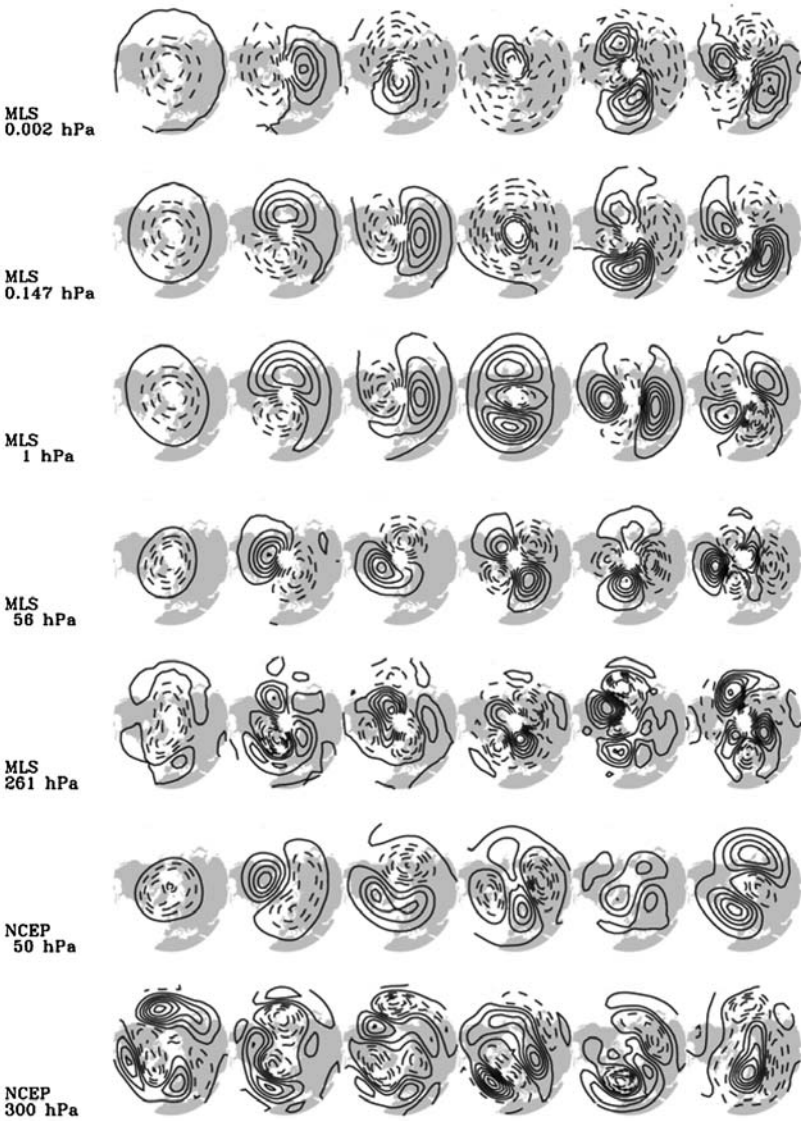

Figure 1. NAM patterns for boreal winter (DJF) at 0.002 hPa, 0.147 hPa, 1 hPa, 56 hPa, and 261 hPa to the minimum latitude of 20N in the azimuthal projection. The solid contours represent the positive values from zero, and dashed contours are negative values. Contour interval is 0.02. The patterns from MLS are calculated as the first six EOFs of MLS daily geopotential height for 2004–2009. NAM patterns for winter (DJF) from monthly averaged NCEP/NCAR reanalysis (1948–2008) are also shown at 50 hPa and 300 hPa.

of area weighted GPH anomalies during DJF months in 2004–2009, at each pressure level.

3. Results and Discussions

3.1. Structures of the Wintertime NAM

[7] Figure 1 shows the first six EOF patterns for the NH winter at selected pressure levels. The first mode appears to be robust and significant at all MLS pressure levels. According to the criterion of *North et al.* [1982], the eigenvalues (λ_k) of the EOF modes have sampling uncertainties $\Delta\lambda_k \sim \lambda_k\sqrt{2/N}$ when the covariance matrix is constructed on the basis of N independent samples ($N \sim 433$). The spacing from first to second mode is greater than this sampling uncertainty at all MLS pressure levels. The pattern of the first mode near the surface, known as an Arctic Oscillation (AO), has higher amplitudes at the polar region and the well-known dipole structure in which the subtropics have the opposite sign from the polar regions [*Thompson and Wallace*, 1998]. However, the patterns of the first EOF in the stratosphere and in the mesosphere have the same sign throughout the northern hemisphere, with amplitudes higher in the pole and decreasing towards the low latitudes. The second and third EOF modes have a higher variance over the persistent Aleutian High which is anti-correlated with the variability over the Icelandic Low. The second and third modes can be viewed as a pair of wave 1 patterns with the orthogonal orientation rotating slightly with altitude. Not well separated, these two modes are ranked consistently at all altitudes in the second and third place in terms of variance contribution. Similar rank has been noted in third and fourth modes of NH column ozone [*Jiang et al.*, 2008]. Details of the first and second modes in the troposphere and the stratosphere, and the

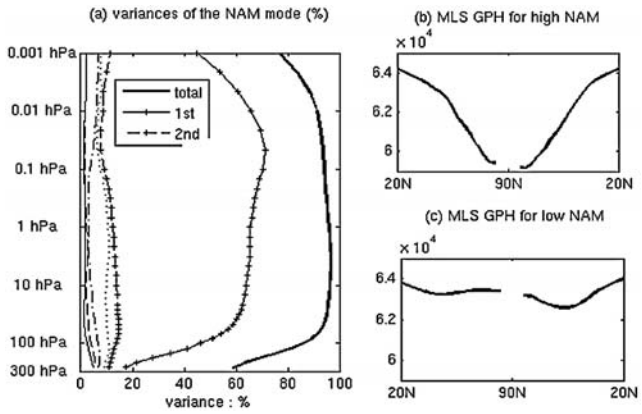

Figure 2. (a) Variance of the each mode of boreal winter (DJF) NAM patterns and integrated total variance of the first seven modes. The patterns are calculated as the first and higher EOFs of daily geopotential height for 2004–2009. The cross sections of the MLS GPH across 90W to 90E for (b) high NAM index and (c) low NAM index at 0.1 hPa in the winter period (DJF). To derive these composite patterns, 69 days above one standard deviation of the NAM index and 55 days below one standard deviation of the index are averaged, respectively.

comparison of the characteristics of these modes with the GCM is discussed by *Lee et al.* [2008]. The comparison of patterns derived from the 5-year MLS record and those from the 57-year NCEP/NCAR reanalysis (Figure 1) show consistent patterns, suggesting that the NAM signals are comparable independent of the length of the record used in the analysis.

[8] The relative importance of the leading EOF modes of MLS wintertime GPH variability is shown in Figure 2a in terms of percentage of variance contribution. The sum of the first six modes accounts for up to 95 percent of the total variance of the geopotential height field in the mesosphere. The first NAM pattern explains more than 65% of the wintertime variance at all levels between 0.01 and 10 hPa. Propagating planetary and gravity waves that reach the mesosphere have amplitudes that grow with height, becoming the dominant dynamical forcing in the upper mesosphere. Since waves are associated with a broad spectrum of variability, the dominance of wave forcings reduces the percentage of variance captured by the first mode. In the high-latitude mesosphere, the amplitudes of gravity waves are at least as significant as those of quasi-stationary planetary waves, such as tides [e.g., *Offermann et al.*, 2009]. Similarly, the upper tropospheric NAM minimum at 316 hPa, with less than 20% of the total variance, is likely associated with large amplitudes of small-scale variability, such as gravity waves [e.g., *Namboothiri et al.*, 2008].

[9] The percentages of the AO, derived from the longer-term monthly NCEP data, are slightly higher than that of the mode in the upper troposphere from the daily MLS data from a relatively short period: 21% from a 57-year analysis [*Lee and Hameed*, 2007], 23% from 40 years of five levels data [*Baldwin and Dunkerton*, 1999], and 22% from 97 years of sea level pressure data [*Thompson and Wallace*, 1998]. Because the first modes at 300–500 hPa account for ~4% less than those near the surface in the NCEP DJF analysis, the 17% of variance at 316 hPa from MLS is comparable to the variances estimated from long term analysis.

[10] In the stratosphere up to 10 hPa, the NAM accounts for substantially more (by about 20%) variance in the MLS data than what was reported by *Lee and Hameed* [2007] from the NCEP/NCAR reanalysis. This is likely caused by greater variability from additional forcing factors, such as decadal variability, volcanic eruptions, and anthropogenic impact, which tend to reduce the contribution of the stratospheric NAM from the long term analysis. The first three leading modes of SLP from a 200-year simulation with the Canadian Centre for Climate Modelling and Analysis (CCCma) model [*Fyfe et al.*, 1999] account for similar variances (24%, 11%, and 9% of the total variance, respectively) to those of the present study.

[11] Figures 2b and 2c illustrate the different patterns of the NAM mode in extremely positive and negative phases. Variations between phases may occur within the same winter or from year to year. In the positive phase, GPH in the mesosphere decreases poleward with a well-like shape centered on the pole, indicating a strong polar vortex in the winter middle atmosphere [*Limpasuvan et al.*, 2005; *Kuroda*, 2008] with strong descent inside the mesospheric portion of the vortex. In this case, GPH variability is a manifestation that, to the first order, the polar winter atmosphere is in radiative equilibrium [*Shepherd*, 2007]. The cold anomaly on the stratosphere means that this region is "closer than normal" to radiative equilibrium without dynamic forcing. The low-index NAM pattern is characterized by a shallow, less-defined GPH well with a weak vortex, which may have multiple minima at midlatitudes. In the low NAM phase with a warm anomaly, the polar atmosphere is "farther than normal" from the radiative equilibrium because of the dynamic forcing. During the prime SSW phase, when the NAM is strongly negative, the polar vortex is associated with a strong descent in the stratosphere but not much in the mesosphere as indicated in MLS trace gas measurements (not shown). However, in the decaying stage of the SSW, the polar vortex starts to form in the mesosphere, showing a strong descent there but not much in the stratosphere.

3.2. NAM Signal in the Middle Atmosphere

[12] Recent works show that there is large variability in winter middle atmosphere during the Aura MLS observation period [e.g., *Siskind et al.*, 2007; *Manney et al.*, 2008; *Coy et al.*, 2009]. Two unusually strong major SSWs occurred in 2006 (wavenumber 1) and in 2009 (wavenumber 2), followed by anomalous cooling in the upper stratosphere [e.g., *Manney et al.*, 2008, 2009a]. Major SSWs resulted in an abrupt increase in stratospheric temperatures, during which the polar vortex was distorted in a downward-progressive development, and shifted off the pole in 2006 but split in 2009.

[13] The EOF analysis provides a powerful tool to extract the dominant patterns in the middle atmospheric dynamics. As seen in Figure 3, there is clear interannual variability in the wintertime stratospheric and mesospheric NAM. Positive NAM, is found in the lower mesosphere and the upper stratosphere between December 2004 and early January 2005, corresponding to strong polar vortex and low temperature anomaly in this height region. This positive phase

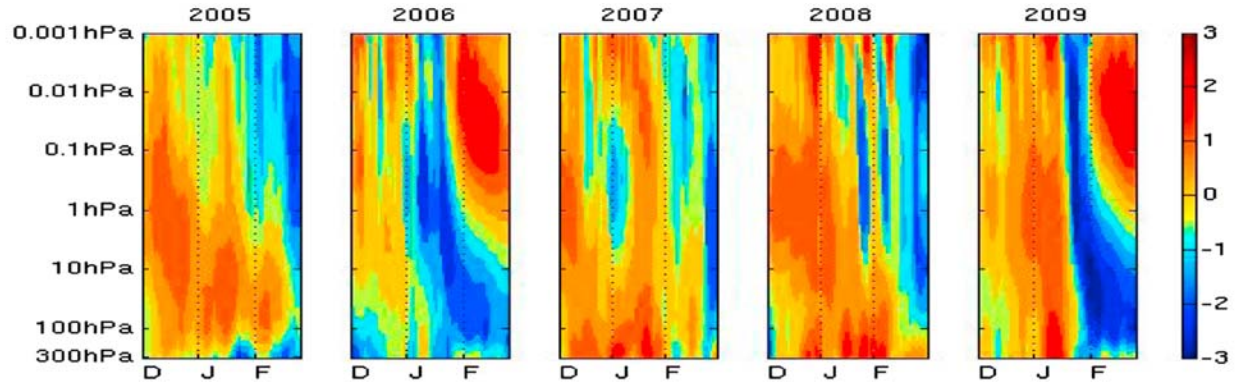

Figure 3. Time-height development of the first mode during boreal winters of 2005–2009. The NAM indexes are normalized with the standard deviation of the indexes to highlight the relative importance of this mode across all altitudes. Red represents positive index (a cold condition with a strong polar vortex) and blue represents negative index (a warm condition with a weak polar vortex).

continues until late February 2005, providing a favorable cold condition for forming polar stratospheric clouds [*Rex et al.*, 2006] in the lower stratosphere. In contrast, strong and persistent negative phases of the NAM are dominant in the mesosphere during January 2006 and 2009. Both winters are characterized by a weakened mesospheric polar vortex with significant easterly anomalies extending down to the upper stratosphere in January.

[14] The negative NAM phases in January 2006 and 2009, associated with easterly zonal wind anomalies in the stratosphere, signal the major SSWs which are characterized by a very rapid increase (~40 K) of the stratospheric polar temperature maximum at 10 hPa for more than two weeks. During 2006 and 2009, the rapid changes of the mesospheric NAM to positive in February capture the fast, strong reformation of the vortex after the warming. The positive NAM patterns are initiated in the mesosphere in late January and progress gradually into the upper stratosphere in February. In both years, the negative phases in the stratosphere persist throughout February in the middle to lower stratosphere. The progression of the mesosphere-to-stratosphere NAM captures the relatively slow recovery of the middle and lower stratospheric vortex after the warming. Vertical coupling of the upper-troposphere, stratosphere, and mesosphere is also observed during February of 2008 brief warming by *Flury et al.* [2009].

[15] In the middle atmosphere, the NAM is a manifestation of the strength of the polar vortex, and its variability is thus largely driven by the wave forcing. In mid January of 2006 and early January of 2009, when the major stratospheric warmings begin, a strong positive phase had also developed in the mesosphere in the second and third EOF modes (not shown). This positive phase indicates the strengthening of the wave 1 in response due to forcing from the troposphere [*Manney et al.*, 2008, 2009a]. In contrast, strong negative phases in the decaying stage of the warming period in 2006 and 2009 Februaries indicate that the vortex is reforming in the mesosphere as the wave 1 response is no longer being forced from the troposphere.

4. Conclusions

[16] The Aura MLS GPH data from mid-2004 to present provide new observations with which to characterize the spatial pattern and temporal evolution of the NAM in the entire middle atmosphere. Daily MLS GPH data is analyzed to extract the first six EOF modes of the middle atmospheric variability and their interannual variations during the boreal winter. The mode from MLS temperature (not shown) appears to be consistent with the results expected from the vertical derivative of GPH, showing high index values in the regions where the GPH vertical gradient is large.

[17] During the winter, the NAM is the most robust mode throughout the middle atmosphere from the upper troposphere to the mesosphere. The NAM dominance between 100 hPa and 0.01 hPa is a manifestation of a predominately radiatively-controlled polar middle atmosphere with the upper boundary near the mesopause. The lower boundary of the middle-atmospheric NAM, characterized by a minimum (17%) variance, is close to the tropopause.

[18] The second and third EOF modes are a pair of orthogonal wave 1 patterns, reflecting the strength of large scale dynamic forcing from the lower atmosphere together with other higher EOF modes. The patterns derived from 5 years of daily MLS data are comparable to those obtained from the longer-term analysis, suggesting that the first three modes are largely independent of the length of data record. SSWs are captured as large anomalies in the EOF modes. Anomaly patterns in the time-height development of the NAM index reveal downward progression from the middle mesosphere to stratosphere. During multiple weeks during SSWs, in both 2006 and 2009, mesospheric cooling up to 20 K is observed by MLS in polar (60N–84N) temperature from 0.01 hPa to 0.2 hPa. In 2006 warming, significant negative NAM signals appear in the mesosphere at early January, but they appear after mid-January in the stratosphere below 10 hPa.

[19] The EOF modes in the mesosphere and their interactions with the stratosphere require further investigations. The MLS observations support the view that the NAM structures in the stratosphere and mesosphere are controlled by a closely coupled system. The MLS observations in the entire middle atmosphere provide a comprehensive view of dynamical links between the lower and upper atmospheres. Large disturbances in the mesosphere often influence the entire stratosphere, and propagate further down to the surface via the stratosphere-troposphere coupling mechanism

[*Holton et al.*, 1995]. These dynamical processes can affect transport and chemistry of atmospheric constituents, e.g., ozone, H_2O, and CO. Details on the processes of transport and chemistry of atmospheric constituents including implications for stratospheric ozone loss will be discussed in the future work.

[20] **Acknowledgments.** We thank the MLS Science Team for their continuing support, especially Jung H. Chae, and Robert P. Thurstans. We also thank to Kirstin Krüger, Varavut Limpasuvan, Alexander Ruzmaikin, Joan Feynman for inspiring discussions and two anonymous reviewers for suggestions and comments that have lead to significant improvements of the paper. This research was supported by an appointment to the NASA Postdoctoral Program at the Jet Propulsion Laboratory, administered by Oak Ridge Associated Universities through a contract with NASA. Research at the Jet Propulsion Laboratory, California Institute of Technology, is done under contract with the National Aeronautics and Space Administration.

References

Baldwin, M. P., and T. J. Dunkerton (1999), Downward propagation of the Arctic Oscillation from the stratosphere to the troposphere, *J. Geophys. Res.*, *104*, 30,937–30,946, doi:10.1029/1999JD900445.

Baldwin, M. P., and T. J. Dunkerton (2001), Stratospheric harbingers of anomalous weather regimes, *Science*, *294*, 581–584, doi:10.1126/science.1063315.

Black, R. X. (2002), Stratospheric forcing of surface climate in the Arctic Oscillation, *J. Clim.*, *15*, 268–277, doi:10.1175/1520-0442(2002)015<0268:SFOSCI>2.0.CO;2.

Brasseur, G., and S. Solomon (2005), *Aeronomy of the Middle Atmosphere*, 3rd ed., Springer, Dordrecht, Netherlands.

Coy, L., S. Eckermann, and K. Hoppel (2009), Planetary wave breaking and tropospheric forcing as seen in the stratospheric sudden warming of 2006, *J. Atmos. Sci.*, *66*, 495–507, doi:10.1175/2008JAS2784.1.

Flury, T. K., et al. (2009), Ozone depletion, water vapor increase, and PSC generation at midlatitudes by the 2008 major stratospheric warming, *J. Geophys. Res.*, *114*, D18302, doi:10.1029/2009JD011940.

Fyfe, J. C., G. J. Boer, and G. M. Flato (1999), The Arctic and Antarctic oscillations and their projected changes under global warming, *Geophys. Res. Lett.*, *26*, 1601–1604, doi:10.1029/1999GL900317.

Hardiman, S. C., and P. H. Haynes (2008), Dynamical sensitivity of the stratospheric circulation and downward influence of upper level perturbations, *J. Geophys. Res.*, *113*, D23103, doi:10.1029/2008JD010168.

Hoffmann, P., W. Singer, and D. Keuer (2002), Variability of the mesospheric wind field at middle and Arctic latitudes in winter and its relation to stratospheric circulation disturbances, *J. Atmos. Sol. Terr. Phys.*, *64*, 1229–1240, doi:10.1016/S1364-6826(02)00071-8.

Hoffmann, P. W., et al. (2007), Latitudinal and longitudinal variability of mesospheric winds and temperatures during stratospheric warming events, *J. Atmos. Sol. Terr. Phys.*, *69*, 2355–2366, doi:10.1016/j.jastp.2007.06.010.

Holton, J. R., et al. (1995), Stratosphere-troposphere exchange, *Rev. Geophys.*, *33*, 403–439, doi:10.1029/95RG02097.

Jiang, X., et al. (2008), Interannual variability and trends of extratropical ozone. Part I: Northern Hemisphere, *J. Atmos. Sci.*, *65*, 3013–3029, doi:10.1175/2008JAS2665.1.

Kuroda, Y. (2008), Effect of stratospheric sudden warming and vortex intensification on the tropospheric climate, *J. Geophys. Res.*, *113*, D15110, doi:10.1029/2007JD009550.

Kushner, P. J., and L. M. Polvani (2004), Stratosphere–troposphere coupling in a relatively simple AGCM: The role of eddies, *J. Clim.*, *17*, 629–639, doi:10.1175/1520-0442(2004)017<0629:SCIARS>2.0.CO;2.

Lahoz, W. A., et al. (2009), Mesosphere–stratosphere transport during Southern Hemisphere autumn deduced from MIPAS observations, *Q. J. R. Meteorol. Soc.*, *135*, 681–694, doi:10.1002/qj.397.

Lee, J. N., and S. Hameed (2007), The Northern Hemisphere annular mode in summer: Its physical significance and its relation to solar activity variations, *J. Geophys. Res.*, *112*, D15111, doi:10.1029/2007JD008394.

Lee, J. N., S. Hameed, and D. T. Shindell (2008), The northern annular mode in summer and its relation to solar activity variations in the GISS ModelE, *J. Atmos. Sol. Terr. Phys.*, *70*, 730–741, doi:10.1016/j.jastp.2007.10.012.

Limpasuvan, V., and D. L. Hartmann (2000), Wave-maintained annular modes of climate variability, *J. Clim.*, *13*, 4414–4429, doi:10.1175/1520-0442(2000)013<4414:WMAMOC>2.0.CO;2.

Limpasuvan, V., et al. (2005), Stratosphere-troposphere evolution during polar vortex intensification, *J. Geophys. Res.*, *110*, D24101, doi:10.1029/2005JD006302.

Manney, G. L., et al. (2008), The evolution of the stratopause during the 2006 major warming: Satellite data and assimilated meteorological analyses, *J. Geophys. Res.*, *113*, D11115, doi:10.1029/2007JD009097.

Manney, G. L., et al. (2009a), Aura Microwave Limb Sounder observations of dynamics and transport during the record-breaking 2009 stratospheric major warming, *Geophys. Res. Lett.*, *36*, L12815, doi:10.1029/2009GL038586.

Manney, G. L., et al. (2009b), Satellite observations and modelling of transport in the upper troposphere through the lower mesosphere during the 2006 major stratospheric sudden warming, *Atmos. Chem. Phys. Discuss.*, *9*, 9693–9745.

Namboothiri, S. P., et al. (2008), CHAMP observations of global gravity wave fields in the troposphere and stratosphere, *J. Geophys. Res.*, *113*, D07102, doi:10.1029/2007JD008912.

North, G. R., T. L. Bell, R. F. Cahalan, and F. J. Moeng (1982), Sampling errors in the estimation of empirical orthogonal functions, *Mon. Weather Rev.*, *110*, 699–706, doi:10.1175/1520-0493(1982)110<0699:SEITEO>2.0.CO;2.

Offermann, D., et al. (2009), Relative intensities of middle atmosphere waves, *J. Geophys. Res.*, *114*, D06110, doi:10.1029/2008JD010662.

Plumb, R. A., and K. Semeniuk (2003), Downward migration of extratropical zonal wind anomalies, *J. Geophys. Res.*, *108*(D7), 4223, doi:10.1029/2002JD002773.

Rex, M., et al. (2006), Arctic winter 2005: Implications for stratospheric ozone loss and climate change, *Geophys. Res. Lett.*, *33*, L23808, doi:10.1029/2006GL026731.

Schwartz, M. J., et al. (2008), Validation of the Aura Microwave Limb Sounder temperature and geopotential height measurements, *J. Geophys. Res.*, *113*, D15S11, doi:10.1029/2007JD008783.

Shepherd, T. G. (2007), Transport in the middle atmosphere, *J. Meteorol. Soc. Jpn.*, *85B*, 165–191, doi:10.2151/jmsj.85B.165.

Sherhag, R., K. Labitzke, and F. G. Finger (1970), Developments in stratospheric and mesospheric analyses which dictate the need for additional upper air data, *Meteorol. Monogr.*, *11*, 85–90.

Siskind, D. E., S. D. Eckermann, L. Coy, and J. P. McCormack (2007), On recent interannual variability of the Arctic winter mesosphere: Implications for tracer descent, *Geophys. Res. Lett.*, *34*, L09806, doi:10.1029/2007GL029293.

Thompson, D. W. J., and J. M. Wallace (1998), The Arctic Oscillation signature in the wintertime geopotential height and temperature fields, *Geophys. Res. Lett.*, *25*, 1297–1300, doi:10.1029/98GL00950.

Thompson, D. W. J., and J. M. Wallace (2000), Annular modes in the extratropical circulation. Part I: Month-to-month variability, *J. Clim.*, *13*, 1000–1016, doi:10.1175/1520-0442(2000)013<1000:AMITEC>2.0.CO;2.

J. N. Lee, G. L. Manney, M. J. Schwartz, and D. L. Wu, Jet Propulsion Laboratory, California Institute of Technology, MS 169-237, 4800 Oak Grove Dr., Pasadena, CA 91109, USA. (jae.nyung.lee@jpl.nasa.gov)